Singularly Perturbed Algorithms for Velocity Consensus and Shape Control of Single Integrator Multi-Agent Systems ⋆

Mohammad Deghat * **Zhiyong Sun** ** **Dragan Nešić** *
Chris Manzie *

* *Department of Electrical and Electronic Engineering, The University of Melbourne, Parkville, 3010, Victoria, Australia.*
(e-mail: {m.deghat; dnesic; manziec}@unimelb.edu.au)
** *Research School of Engineering, Australian National University, Canberra, Australia. Now with Department of Automatic Control, Lund University, Sweden. (e-mail: sun.zhiyong.cn@gmail.com)*

Abstract: This paper studies a distributed multi-agent control problem in which the agents have single-integrator dynamics. A distributed control law is proposed to drive the agents to attain a desired formation shape and acquire an identical velocity. Using singular perturbation theory and stability results for nonlinear cascade systems, it is shown that agents can achieve the desired formation shape and velocity at different time scales. Moreover, it is shown that there exists an upper bound for a time-scale parameter (perturbation parameter) in the control law such that for time-scale parameters less than this bound, the initial conditions of the shape control error system will remain in a stability basin of the equilibrium. Simulation results are provided to validate the proposed algorithm.

Keywords: Multi-agent system, consensus, formation shape control, singular perturbation.

1. INTRODUCTION

The problems of consensus and formation shape control are two of the most fundamental and widely concerned problems in distributed multi-agent control. The goal in the consensus problem is to control agents in a distributed manner to assume a common state (for example a common velocity) using the states of their neighbor agents. A comprehensive treatment of consensus methods can be found in e.g. Olfati-Saber et al. (2007); Ren et al. (2007); Mesbahi and Egerstedt (2010). In the formation shape control problem, it is common to use distributed gradient-based control algorithms which are designed so that the agents in a formation cooperatively achieve a specified desired shape; see Krick et al. (2009); Oh et al. (2015) for more information.

The goal in this paper is to study the combined problem of velocity consensus and shape control. This problem has been studied in Olfati-Saber (2006); Tanner et al. (2007); Dimarogonas and Johansson (2008) and recently in more details in Deghat et al. (2016); Sun et al. (2017) for systems with double-integrator dynamics, where the control algorithm sets the acceleration for each agent. The idea in the above-mentioned papers is to design a distributed control law as the sum of the gradient-based shape control law and the linear velocity consensus algorithm. We, however, aim in this paper to control agents with *single-integrator dynamics*; so the control law sets the velocity for each agent.

⋆ The work of M. Deghat, D. Nešić and C. Manzie is supported by the ARC Discovery Project, grant number DP170104102.

An advantage of the proposed control algorithm is that the velocity consensus and formation shape control objectives can be obtained at different time-scales. This, however, could not be obtained for double-integrator systems in the above-mentioned papers.

As is common in the above-mentioned results for double-integrator systems, we also assume the structure of the graphs associated with shape control and consensus are not necessarily identical. In other words, an agent might aim to achieve a desired inter-agent distance to one of its neighbors while does not try to assume a common velocity with that agent, and vice versa. Coordination control of multi-agent systems with generalized graph topologies between shape control and velocity control will enable more freedoms in designing interaction graphs, as shown in Qin et al. (2012). Having two different graphs for velocity consensus and shape control will result in less communications/measurements between the neighbor agents, and is not possible, for example, in Cao et al. (2010); Deghat et al. (2015) where sliding mode control laws are used to control the agents.

The stability analysis is carried out using stability results for nonlinear cascade systems and also singular perturbation arguments, guaranteeing exponential convergence of velocity consensus and shape control error to zero.

2. BASIC NOTATION AND BACKGROUND

2.1 Notation

Consider a multi-agent system with n agents in $\mathbb{R}^2$, with the i-th agent located at p_i. The agents are assumed to have single-integrator dynamics

$$u_i = \dot{p}_i, \tag{1}$$

where $u_i \in \mathbb{R}^2$ is the control input applied to agent i. Define $p \in \mathbb{R}^{2n}$ as a column vector of all agent positions stacked together. Likewise, $u \in \mathbb{R}^{2n}$ denotes the vector of all u_i stacked together. In this paper, we consider a formation in the 2-D space, while the derived results can be readily extended to higher dimensional spaces.

For formation control purposes, consider a graph $\mathcal{G}_s = (\mathcal{V}_s, \mathcal{E}_s)$ with n vertices and m edges where $\mathcal{V}_s$ is a list of vertices, one corresponding to each agent, and $\mathcal{E}_s \subset \mathcal{V}_s \times \mathcal{V}_s$ is a list of agent pairs (edges of the graph) labeled $1, 2, \cdots, m$. There is an edge in $\mathcal{E}_s$ from vertex i to vertex j $(i, j \in \mathcal{V}_s)$, when agent j can measure its relative position to agent i. We assume in this paper that the formation control graph is undirected, that is if there is an edge from vertex i to vertex j, then there is also an edge from vertex j to vertex i. The neighbor set $\mathcal{N}_i$ of node i is defined as $\mathcal{N}_i = \{j \in \mathcal{V}_s : (i, j) \in \mathcal{E}_s\}$.

Define $d_{k_{ij}} = \|p_i - p_j\|$ as the length of edge k linking agents i and j, and $d^*_{k_{ij}}$ as the desired or specified distance between the same agents; we may later use d_k and d^*_k instead of $d_{k_{ij}}$ and $d^*_{k_{ij}}$ for notational convenience when no confusion arises. The incidence matrix H_s is an $n \times m$ matrix that relates the nodes of $\mathcal{G}_s$ to its edges and is defined as $H_s = [h^s_{ij}]$, where

$$h^s_{ij} = \begin{cases} -1 & \text{if the } j\text{-th edge sinks at node i;} \\ 1 & \text{if the } j\text{-th edge leaves node i;} \\ 0 & \text{otherwise.} \end{cases} \tag{2}$$

Note that the incidence matrix has a column sum equal to zero, i.e. $\ker(H_s^\top) = \text{span}\{\mathbf{1}\}$, where $\mathbf{1}$ denotes a vector of all 1's; see Mesbahi and Egerstedt (2010). We define $\mathcal{H}_s$ as $\mathcal{H}_s := H_s \otimes I_2$ where $\otimes$ denotes the Kronecker product of matrices.

For the velocity consensus purpose, let $\mathcal{G}_v = (\mathcal{V}_v, \mathcal{E}_v)$ denote a graph governing the information transmission between pairs of agents. There is an edge in $\mathcal{E}_v$ from vertex i to vertex j $(i, j \in \mathcal{V}_v)$, when agent j can receive signals from agent i. The neighbor set $\overline{\mathcal{N}}_i$ denotes the set of agents $k \in \mathcal{V}_v$ supplying information to agent i. Let $L_v = [l^v_{ij}]$ denote the Laplacian matrix associated with $\mathcal{G}_v$; for $i \neq j$, there holds $l^v_{ij} = -1$ if and only if there is an edge from j to i, and $l^v_{ij} = 0$ otherwise. Moreover, $l^v_{ii} = -\sum_j l^v_{ij}$. We define $\mathcal{L}_v$ as $\mathcal{L}_v := L_v \otimes I_2$. For an *undirected graph*, L_v can be written as $L_v = H_v H_v^\top$, where H_v is the incidence matrix associated with $\mathcal{G}_v$ and has the property that $H_v^\top \mathbf{1} = 0$.

2.2 Graph rigidity

We briefly summarize the concept of graph rigidity in this subsection; see Hendrickx et al. (2007); Anderson et al. (2008) for more information. Rigidity is a property that refers to undirected graphs. A *framework* is defined as a graph $\mathcal{G}_s = (\mathcal{V}_s, \mathcal{E}_s)$ with n vertices and m edges together with a set of points p that map $\mathcal{V}_s$ to $\mathbb{R}^{2n}$. We denote such a framework by the pair $(\mathcal{G}_s, p)$. Let the formation control graph $\mathcal{G}_s = (\mathcal{V}_s, \mathcal{E}_s)$ with n vertices and m edges be undirected. Two frameworks $(\mathcal{G}_s, p)$ and $(\mathcal{G}_s, \bar{p})$ are *congruent* if for each pair of distinct labels $i, j \in \{1, \cdots, n\}$, $\|p_i - p_j\| = \|\bar{p}_i - \bar{p}_j\|$. *Rigidity* means that if a formation is such that at some time t there holds $\|p_i - p_j\| = d^*_{k_{ij}}$ for all $(i, j) \in \mathcal{E}_s$, then the only continuous motions of the formation are ones which preserve its shape so that the geometric figure after the move must be congruent with that before the move. Roughly speaking, a framework is rigid if it is impossible to deform it by slightly moving its points while preserving all edge length constraints. It is common in most formation shape control problems to assume the set of edges $\mathcal{E}_s$ defined by the distance data ensures that the associated graph $\mathcal{G}_s$ is at least *rigid* and we shall do that too.

Although rigidity is an intuitive concept, the definition of rigidity does not provide a condition that is easy to check. However, there is a *rigidity matrix*, defined below, whose rank will provide conditions on the rigidity of a framework. Define the vector $q \in \mathbb{R}^{2m}$ as

$$q := \mathcal{H}_s^\top p \tag{3}$$

where $q = \left[q_1^\top, \cdots, q_m^\top\right]^\top$. Define the *rigidity function*, $r_{\mathcal{G}_s}(p) : \mathbb{R}^{2n} \to \mathbb{R}^m$ as

$$r_{\mathcal{G}_s}(p) := \frac{1}{2}\left[\|q_1\|^2, \cdots, \|q_m\|^2\right]^\top, \tag{4}$$

which can also be written as $g_{\mathcal{G}_s}(q) : \mathbb{R}^{2m} \to \mathbb{R}^m$. Then the rigidity matrix, $R_{\mathcal{G}_s}(q)$, is defined as

$$R_{\mathcal{G}_s}(q) := \frac{\partial r_{\mathcal{G}_s}(p)}{\partial p} = \frac{\partial g_{\mathcal{G}_s}(q)}{\partial q}\frac{\partial q}{\partial p} = (D(q))^\top \mathcal{H}_s^\top \tag{5}$$

where $D(q) = \text{diag}\{q_1, \cdots, q_m\} \in \mathbb{R}^{2m \times m}$.

A framework in $\mathbb{R}^2$ is *infinitesimally rigid* if the rank of the rigidity matrix is $2n - 3$. Infinitesimal rigidity is a stronger condition than rigidity, i.e. if a framework is infinitesimally rigid, then it is also rigid but the converse is not necessarily true. In order to have an infinitesimally rigid framework, the graph should have at least $2n - 3$ edges. If a framework is infinitesimally rigid in $\mathbb{R}^2$ and has exactly $2n - 3$ edges, then it is called a *minimally and infinitesimally rigid* framework which has the following property.

Lemma 1. (Mou et al. (2016); Sun et al. (2016)).
If a framework $(\mathcal{G}_s, p)$ is minimally and infinitesimally rigid in $\mathbb{R}^2$, then the matrix $R_{\mathcal{G}_s}(q)R^\top_{\mathcal{G}_s}(q)$ is positive definite.

Note the above lemma also holds for $\mathbb{R}^d$ ($d \in \mathbb{N}_+$ with $d > 2$) space case, and again the main results can be extended to higher dimensional spaces. In this paper, we use the two terms *framework* and *formation* interchangeably. We will mainly deal with formations which are either rigid or minimally and infinitesimally rigid. Rigidity is defined for frameworks, however rigidity is a generic property, that is, a property which holds true for frameworks with generic agent positions. Therefore, by slight abuse of notation, we also say a graph $\mathcal{G}_s$ is rigid if a framework $(\mathcal{G}_s, p)$ is generically rigid. We make the following assumption.

Assumption 1. The velocity consensus graph $\mathcal{G}_v$ is undirected and connected and the formation control graph $\mathcal{G}_s$ is undirected and rigid.

3. MAIN RESULT

3.1 The proposed control law

Define the potential function $V(p)$ as

$$V(p) = \frac{1}{4}\sum_{(i,j)\in\mathcal{E}_s}\left(\|p_i - p_j\|^2 - d_{k_{ij}}^{*2}\right)^2, \tag{6}$$

and observe that $V(p) = 0$ at the desired formation shape and is positive otherwise. Notice that this expression is invariant under translation, rotation or reflection of the formation. Define $\mathrm{d}^* \in \mathbb{R}^m$ as

$$\mathrm{d}^* = \frac{1}{2}\left[d_1^{*2}, \cdots, d_m^{*2}\right]^\top. \tag{7}$$

We aim to control the agents such that the trajectories $(p, \dot{p})$ tend as $t \to \infty$ to the set

$$\Omega_p = \left\{(p, \dot{p}) \mid r_{\mathcal{G}_s}(p) = \mathrm{d}^*,\ \dot{p} = \mathrm{span}\{\mathbf{1}\}\right\}. \tag{8}$$

To this end, we propose the following control law,

$$u_i = \sum_{j\in\mathcal{N}_i}(p_j - p_i)\left(\|p_i - p_j\|^2 - d_{k_{ij}}^{*2}\right) + z_i, \tag{9a}$$

$$\varepsilon\dot{z}_i = \sum_{k\in\overline{\mathcal{N}}_i}(z_k - z_i), \tag{9b}$$

where ε is a positive time-scale parameter and z_i, $i = 1, \cdots, n$ is an internal state of the system. As defined earlier, the neighborhood sets $\mathcal{N}_i$ and $\overline{\mathcal{N}}_i$ correspond respectively to the formation control graph $\mathcal{G}_s$ and velocity consensus graph $\mathcal{G}_v$. The above control laws can be written in the compact form

$$u = -\nabla V(p) + z, \tag{10a}$$

$$\varepsilon\dot{z} = -\mathcal{L}_v z, \tag{10b}$$

where z is the vector of all z_i stacked together. From (1) and (10), the closed-loop system can be written as

$$\dot{p} = -\nabla V(p) + z, \tag{11a}$$

$$\varepsilon\dot{z} = -\mathcal{L}_v z. \tag{11b}$$

Remark 1. The conventional double-integrator formation control model represented in Deghat et al. (2016); Sun et al. (2017) is

$$\dot{p} = \nu \tag{12a}$$

$$\dot{\nu} = u = -\mathcal{L}_v\nu - \nabla V(p) \tag{12b}$$

where ν is the velocity vector of all agents stacked together. To distinguish between the single-integrator model (11) and the double-integrator model (12), note that in the double-integrator model, we control the agents' accelerations while in the single-integrator case we control the agent's velocities. Moreover, as shown in Deghat et al. (2016), it is not easy in the conventional double-integrator model (12) to have a two-time-scale behavior, even when the consensus term is multiplied by a large gain k. This, however, can be easily obtained for the proposed single-integrator model (11) by making the control parameter $\varepsilon > 0$ small.

The different time scales in the proposed model (11) can be interpreted as follows. The consensus subsystem (11b) involves communication or computation between individual agents which thus enables a fast dynamics. On the contrast, the formation shape subsystem (11a) usually involves physical motions among individual agents, which often evolve in a much slower time scale. The differences in such time scales can be captured by the parameter $\varepsilon > 0$ in the proposed system (11).

3.2 Coordinate transformation

The set Ω_p defined in (8) is not a compact set which complicates the stability analysis of the closed-loop system. So we will propose a set parametrized in the link space q which is compact. To this end, we perform the following change of coordinates. Define $e_{k_{ij}}$ as

$$e_{k_{ij}} := \|p_i - p_j\|^2 - d_{k_{ij}}^{*2}. \tag{13}$$

We may later refer to $e_{k_{ij}}$ as e_k for notational convenience if no confusion arises. Define $e \in \mathbb{R}^m$ as

$$e = [e_1, \cdots, e_m]^\top. \tag{14}$$

Then the potential function $V(p)$ defined in (6) can be redefined as

$$V_e(e) = \frac{1}{4}\sum_{k=1}^{m} e_k^2. \tag{15}$$

Define $P \in \mathbb{R}^{2n\times 2n}$ as an orthonormal matrix whose first two rows are $\frac{\mathbf{1}^\top\otimes I_2}{\sqrt{n}}$ and define $\bar{z}$ as

$$\bar{z} := Pz. \tag{16}$$

Then the closed-loop system (11) can be written as

$$\begin{aligned}\dot{e} &= \frac{\partial e}{\partial p}\dot{p}\\ &= 2R_{\mathcal{G}_s}(q)\left(-\frac{\partial V(p)}{\partial p} + P^\top\bar{z}\right)\\ &= -2R_{\mathcal{G}_s}(q)\left(\frac{\partial e}{\partial p}\right)^\top\frac{\partial V_e(e)}{\partial e} + 2R_{\mathcal{G}_s}(q)P^\top\bar{z}\\ &= -2R_{\mathcal{G}_s}(q)R_{\mathcal{G}_s}^\top(q)e + 2R_{\mathcal{G}_s}(q)P^\top\bar{z}, \end{aligned} \tag{17a}$$

$$\varepsilon\dot{\bar{z}} = -P\mathcal{L}_v P^\top\bar{z}. \tag{17b}$$

The Laplacian matrix has the property that $L_v\mathbf{1} = 0$ and thus $\mathcal{L}_v(\mathbf{1}\otimes I_2) = 0$. Since $\mathcal{G}_v$ is connected according to Assumption 1, the matrix $P\mathcal{L}_v P^\top$ has only two zero eigenvalues and the rest are positive. Moreover, since $\mathcal{G}_v$ is assumed to be undirected, the Laplacian matrix L_v can be written as $L_v = H_v H_v^\top$ where $H_v^\top\mathbf{1} = 0$ and therefore the first two columns of $(H_v^\top\otimes I_2)P^\top$ are zero as the first two rows of P are $\frac{\mathbf{1}^\top\otimes I_2}{\sqrt{n}}$. So the matrix $P\mathcal{L}_v P^\top$ can be partitioned as

$$P\mathcal{L}_v P^\top = \begin{bmatrix} 0_{2\times 2} & 0\\ 0 & \hat{\mathcal{L}}_v\end{bmatrix} \tag{18}$$

where $\hat{\mathcal{L}}_v \in \mathbb{R}^{(2n-2)\times(2n-2)}$ is a symmetric positive definite matrix. Let $\bar{z}$ be partitioned as $\bar{z} = [z^{o\top}\ \hat{z}^\top]^\top$ where z^o is a 2-vector and $\hat{z}$ is a $2n-2$ vector.

Since $\mathcal{H}_s^\top P^\top$ is a $2m\times 2n$ matrix with the first two columns equal to zero, the first two columns of $R_{\mathcal{G}_s}(q)P^\top$, which according to (5) is equal to $(D(q))^\top\mathcal{H}_s^\top P^\top$, is zero and therefore

$$R_{\mathcal{G}_s}(q)P^\top\begin{bmatrix} z^o\\ \hat{z}\end{bmatrix} = R_{\mathcal{G}_s}(q)P^\top\begin{bmatrix} 0\\ \hat{z}\end{bmatrix}. \tag{19}$$

So we conclude that $\dot{e}(t)$ is independent of z^o and (17) can be written as

$$\dot{e} = -2R_{\mathcal{G}_s}(q)R_{\mathcal{G}_s}^\top(q)e + 2R_{\mathcal{G}_s}(q)P^\top \begin{bmatrix} 0 \\ \hat{z} \end{bmatrix} \tag{20a}$$
$$\varepsilon\dot{\hat{z}} = -\hat{\mathcal{L}}_v\hat{z} \tag{20b}$$
$$\varepsilon\dot{z}^o = 0. \tag{20c}$$

Since $\hat{\mathcal{L}}_v$ is positive definite, we conclude that $\hat{z}$ converges to zero exponentially fast for any given $\varepsilon > 0$.

3.3 Singular perturbation analysis

The singular perturbation theory can be used to analyze the stability of (20) via the behavior of two auxiliary systems, namely the reduced (slow) system and the boundary layer (fast) system. Letting $\varepsilon = 0$, the differential equation (20b) degenerates to the algebraic equation

$$\hat{\mathcal{L}}_v\hat{z} = 0 \tag{21}$$

where $\hat{\mathcal{L}}_v$ is positive definite as explained above and therefore $\hat{z} = 0$ is an isolated solution to (21). Then we substitute the solution $\hat{z} = 0$ into (20a) and obtain the *reduced system* as

$$\dot{e}_r = -2R_{\mathcal{G}_s}(q)R_{\mathcal{G}_s}^\top(q)e_r, \tag{22}$$

where the subscript r denotes the state of the reduced system. Note that it was fine not to consider (20c) to calculate the reduced system as (20a) is not a function of z^o and therefore the reduced system is independent of z^o as can be seen in (22).

Define the fast time variable τ as $\tau := t/\varepsilon$. Then the *boundary layer system* is defined as

$$\frac{d\hat{z}_b}{d\tau} = -\hat{\mathcal{L}}_v\hat{z}_b, \qquad \frac{dz_b^o}{d\tau} = 0, \tag{23}$$

and the subscript b denotes the state of the boundary layer system. Later in this section, we use the above reduced and boundary layer systems to study the stability of (20) for small ε.

3.4 Stability analysis

It is well known in the formation control literature that the trajectories of the gradient-based shape control algorithm

$$\dot{p} = u = -\nabla V(p) \tag{24}$$

where $V(p)$ is defined in (6) may converge to different equilibria for different initial conditions. We call the set of equilibria at which the correct shape is attained the *correct* or *desired equilibrium* set, and call other equilibrium points the *undesired equilibrium* points. An example of undesired equilibrium points for (24) with potential function (6) is $p_i = p_j,\ \forall i, j = 1, \cdots, n$, i.e., all agents are collocated. Collinear undesired equilibrium points may also occur; see e.g., Sun et al. (2015).

A target formation is described by a pair $(\mathcal{G}_s, \mathrm{d}^*)$ where d^* is defined in (7) and specifies the target lengths for the edges of $\mathcal{G}_s$.

As explained in Mou et al. (2016), for a target formation $(\mathcal{G}_s, \mathrm{d}^*)$ and each $\bar{p}$ satisfying $\bar{p} = r_{\mathcal{G}_s}^{-1}(\mathrm{d}^*)$, where $r_{\mathcal{G}_s}(\bar{p})$ is defined in (4), there exists an invariant set $\mathcal{A}$ containing $\bar{p}$ such that the rigidity matrix (5) is full row rank for all $p \in \mathcal{A}$. We show in the following theorem that for the system (20), there exists an ε^* and a compact set such that if the initial conditions for p are such that the error e starts in that set, then $e(t)$ stays in the set for $\varepsilon \in (0, \varepsilon^*]$ and for all $t > 0$. The idea for this part of theorem and its proof is taken from Awad et al. (2018).

Theorem 1. Consider a multi-agent system with single-integrator dynamics (1), controlled by a set of distributed controllers (9) and let Assumption 1 hold. Then the following conclusions hold:

(i) For any given $\varepsilon > 0$, any compact sets $D_{\hat{z}} \in \mathbb{R}^{2n-2}$ and $D_e \in \mathbb{R}^m$ that contain the origin and all initial conditions $\hat{z}(0) \in D_{\hat{z}}$ and $e(0) \in D_e$, the signal $\hat{z}(t)$ converges to zero exponentially fast and $e(t)$ converges to the set
$$\Omega_e = \{e \in \mathbb{R}^m : R_{\mathcal{G}_s}^\top(q)e = 0\}$$
as $t \to \infty$.

(ii) Given a target formation $(\mathcal{G}_s, \mathrm{d}^*)$, suppose the framework $(\mathcal{G}_s, p)$ is minimally and infinitesimally rigid at each $p = r_{\mathcal{G}_s}^{-1}(\mathrm{d}^*)$. Then the point $(\hat{z}, e) = (0, 0)$ is locally exponentially stable for all $\varepsilon > 0$.

(iii) Adopt the hypothesis in (ii) and suppose there exists a compact set $\bar{D}_e$ such that for any $e_0 \in \bar{D}_e$, the error $e(t)$ generated by $\dot{p} = -\nabla V(p)$ stays in $\bar{D}_e$. Then there exists a subset $\mathcal{C} : \mathcal{C} \subset \bar{D}_e$ and a parameter $\varepsilon^* > 0$, which depends on $\mathcal{C}$, such that for all $\varepsilon \in (0, \varepsilon^*)$, all trajectories $(\hat{z}(t), e(t))$ starting in $D_{\hat{z}} \times \mathcal{C}$ will remain in $D_{\hat{z}} \times \mathcal{C}$ for all $t > 0$ and will converge to zero exponentially fast as $t \to \infty$.

Proof. (i) Since $\hat{\mathcal{L}}_v$ in (20b) is positive definite, we obtain that $\hat{z}(t)$ converges to zero exponentially fast. To show that $e(t)$ converges to the set Ω_e, we use the following Lyapunov function and then apply LaSalle's invariance principle; see (Sastry, 1999, Proposition 5.22). Define $W(e, \hat{z})$ as

$$W(e, \hat{z}) := (1 - d)V_e(e) + dV_f(\hat{z}), \tag{25}$$

where $V_e(e)$ is defined in (15), $V_f(\hat{z}) := \frac{1}{2}\hat{z}^\top\hat{z}$ and $0 < d < 1$. Then the derivative of W is calculated as follows

$$\begin{aligned}\dot{W} &= (1 - d)\frac{\partial V_e(e)}{\partial e}\dot{e} + d\frac{\partial V_f(\hat{z})}{\partial \hat{z}}\dot{\hat{z}} \\ &\overset{(20)}{=} (1 - d)\left(-e^\top R_{\mathcal{G}_s}(q)R_{\mathcal{G}_s}^\top(q)e + e^\top R_{\mathcal{G}_s}(q)P^\top \begin{bmatrix} 0 \\ \hat{z} \end{bmatrix}\right) \\ &\quad - \frac{d}{\varepsilon}\hat{z}^\top\hat{\mathcal{L}}_v\hat{z}.\end{aligned} \tag{26}$$

Define $\bar{e} = R_{\mathcal{G}_s}^\top(q)e$ and note that $\|P^\top[0\ \hat{z}^\top]^\top\| = \|\hat{z}\|$ as P is an orthonormal matrix. Then (26) can be written as

$$\dot{W} \leqslant -\left[\|\bar{e}\|\ \|\hat{z}\|\right]\bar{Q}\begin{bmatrix}\|\bar{e}\| \\ \|\hat{z}\|\end{bmatrix} \tag{27}$$

where

$$\bar{Q} = \begin{bmatrix} (1 - d) & -\frac{(1-d)}{2} \\ -\frac{(1-d)}{2} & \frac{d}{\varepsilon}\lambda_1(\hat{\mathcal{L}}_v) \end{bmatrix}. \tag{28}$$

and $\lambda_1(\hat{\mathcal{L}}_v)$ denotes the smallest eigenvalue of $\hat{\mathcal{L}}_v$ which is positive according to Assumption 1.

We aim to show that $\bar{Q}$ is positive definite. Since the trace of $\bar{Q}$ is positive, we only need to show that the determinant of $\bar{Q}$ is positive, and $\det(\bar{Q}) > 0$ if

$$\frac{d}{(1 - d)} > \frac{\varepsilon}{4\lambda_1(\hat{\mathcal{L}}_v)}. \tag{29}$$

So for any given $\varepsilon > 0$, we can choose d, which might be close to 1 for small values of ε, such that the above inequality holds.

We now use LaSalles's invariance principle. Define Ω_S as $\Omega_S = \{e \in \mathbb{R}^m, \hat{z} \in \mathbb{R}^{2n-2}:$

$$W(e,\hat{z}) \leqslant c_w := (1-d)\max_{e\in\partial D_e} V_e(e) + d\max_{\hat{z}\in\partial D_{\hat{z}}} V_f(\hat{z})\},$$

where ∂D denotes the boundary of a set D. Since $\bar{Q}$ is positive definite, we obtain from (27) that $\dot{W} = 0$ if and only if $\bar{e} = 0$ and $\hat{z} = 0$. So from LaSalle's invariance principle, all trajectories starting in Ω_S will converge to $\bar{e} = R^\top_{\mathcal{G}_s}(q)e(t) = 0$ and $\hat{z} = 0$. This completes the proof of statement (i).

(ii) The proof follows directly from the standard stability proofs of nonlinear cascade systems; see e.g. Loría and Panteley (2005) and (Terrell, 2009, Chapter 9). Consider the error system (20a) and (20b) and note that (20b) and also the nominal system

$$\dot{e} = -2R_{\mathcal{G}_s}(q)R^\top_{\mathcal{G}_s}(q)e \tag{30}$$

are exponentially stable. We can also conclude from the proof of the first part of the theorem, that $R_{\mathcal{G}_s}(q)$ is bounded when the initial conditions of the error system are in a compact set. So the point $(e,\hat{z}) = (0,0)$ is locally exponentially stable.

(iii) We consider the same Lyapunov function W as (25) with derivative (26). Since the target formation $(\mathcal{G}_s, \mathrm{d}^*)$ is minimally and infinitesimally rigid, there exists $\delta > 0$ such that $R_{\mathcal{G}_s}(q)R^\top_{\mathcal{G}_s}(q)$ is positive definite for all $q \in D_q$ where D_q is defined as

$$D_q = \{q \in \mathbb{R}^{2m} : |g_{\mathcal{G}_s}(q) - \mathrm{d}^*| \leqslant \delta\mathbf{1}\}. \tag{31}$$

Then the first and the third terms on the right hand side of (26) can be bounded by

$$\begin{aligned}&-(1-d)e^\top R_{\mathcal{G}_s}(q)R^\top_{\mathcal{G}_s}(q)e\\ &\qquad\leqslant -(1-d)\|e\|^2 \inf_{q\in D_q}\lambda_1\left(R_{\mathcal{G}_s}(q)R^\top_{\mathcal{G}_s}(q)\right),\\ &-\frac{d}{\varepsilon}\hat{z}^\top\hat{\mathcal{L}}_v\hat{z} \leqslant -\frac{d}{\varepsilon}\|\hat{z}\|^2\lambda_1(\hat{\mathcal{L}}_v).\end{aligned} \tag{32}$$

From (i), we know that $e(t)$ is bounded and therefore $\|q_i\|$ is bounded for all $i = 1,\cdots,m$. Thus, there exists $\beta \geqslant 0$ such that

$$e^\top R_{\mathcal{G}_s}(q)P^\top \begin{bmatrix}0\\ \hat{z}\end{bmatrix} \leqslant \beta\|e\|\|\hat{z}\|. \tag{33}$$

So (26) can be written as

$$\dot{W} \leqslant -\left[\|e\| \ \|\hat{z}\|\right] Q \begin{bmatrix}\|e\|\\ \|\hat{z}\|\end{bmatrix}$$

where

$$Q = \begin{bmatrix}(1-d)\inf_{q\in D_q}\lambda_1\left(R_{\mathcal{G}_s}(q)R^\top_{\mathcal{G}_s}(q)\right) & -\frac{\beta(1-d)}{2}\\ -\frac{\beta(1-d)}{2} & \frac{d}{\varepsilon}\lambda_1(\hat{\mathcal{L}}_v)\end{bmatrix}.$$

We want to find conditions on ε such that Q is positive definite. Since the trace of Q is positive, Q is positive definite if the determinant of Q is also positive, and the determinant is positive if

$$\frac{d}{1-d} > \frac{\varepsilon\beta^2}{4\lambda_1(\hat{\mathcal{L}}_v)\inf_{q\in D_q}\lambda_1\left(R_{\mathcal{G}_s}(q)R^\top_{\mathcal{G}_s}(q)\right)}. \tag{34}$$

Similarly to (Awad et al., 2018, Proof of Theorem III.8), define $v_c = \min_{e\in\partial\bar{D}_e} V_e(e)$ and $r_z = \max_{\hat{z}\in D_{\hat{z}}}\|\hat{z}\|^2$, and define $\mathcal{C} = \{e \mid V_e(e) < v_c\}$.

Choose a sublevel set $\bar{\mathcal{C}} = \{e \mid V_e(e) < v_s\}$ with $\bar{\mathcal{C}} \subset \bar{D}_e$ and $0 \in \bar{\mathcal{C}}$ such that $v_s < v_c$. To make sure that $e(t)$ remains in $\bar{D}_e$, we define the maximum allowable level set of W by the minimum value of $V_e(e)$ on the boundary of $\bar{D}_e$, that is, we assume $W < (1-d)v_c$. Choosing $V_e(e) = v_s$ and $V_f(\hat{z}) = r_z^2$, we obtain

$$(1-d)v_c > (1-d)v_s + \frac{d}{2}r_z^2 \tag{35}$$

and therefore

$$\frac{d}{1-d} < \frac{2(v_c - v_s)}{r_z^2}. \tag{36}$$

Finally from (36) and (34) we have

$$\varepsilon^* < \frac{8(v_c - v_s)\inf_{q\in D_q}\lambda_1\left(R_{\mathcal{G}_s}(q)R^\top_{\mathcal{G}_s}(q)\right)\lambda_1(\hat{\mathcal{L}}_v)}{r_z^2\beta^2}. \qquad \square$$

Remark 2. For the gradient-based formation shape control algorithm (24) with the potential function (6), if agents have certain initial conditions, they might not achieve the desired formation shape. For example, if they are all co-located at $t = 0$ they will stay at their initial locations for $t \geqslant 0$ as $\dot{p}_i(t) = 0$, $\forall t \geqslant 0$ for all agents. However, this might not be the case when the system dynamics is governed by (11). Even if the agents are all co-located at $t = 0$, they might achieve the desired formation shape if the initial conditions of z_i are chosen properly. This control system property can be interpreted by employing the recently developed dimensional-invariance principle in networked systems discussed in Sun and Yu (2017). The proposed control system (11) does not satisfy the condition for ensuring dimensional-invariance property as shown in (Sun and Yu, 2017, Theorem 1); therefore, trajectories of (11) can escape from initially co-located or collinear positions, and this can be a favorable property for formation shape control in practice. This will be demonstrated by a numerical example in the following section.

4. SIMULATIONS

In this section, we numerically analyze the performance of the proposed controller (9) when applied to the single-integrator robots (1). We consider a formation with three agents where all agents are initially at the point $(1,-1)$. We assume the desired formation shape is an equilateral triangle with edge length 1 in $\mathbb{R}^2$, and consider three cases where ε is 0.1, 0.5 and 1. The trajectories of the agents when $\varepsilon = 0.1$ are shown in Fig. 1.

As shown in Fig. 2, the rate of convergence of the velocity consensus increases as ε decreases. It can also be observed in Fig. 2 and Fig. 3 that the steady state error of the velocity consensus and shape control algorithms converge to zero for all ε values as $t \to \infty$. The initial positions of the agents are deliberately chosen to be equal, to show the fact that the agents converge to the desired shape even from such initial positions; see Remark 2. We assumed here that the initial values for z_i are different.

5. CONCLUSIONS

In this paper, we proposed a control law for combined flocking and formation shape control of a multi-agent system with single-integrator dynamics. Aside from the stability results in this paper, an upper bound for the time-scale parameter was obtained that constraints the initial states to be in a stability basin of the equilibrium.

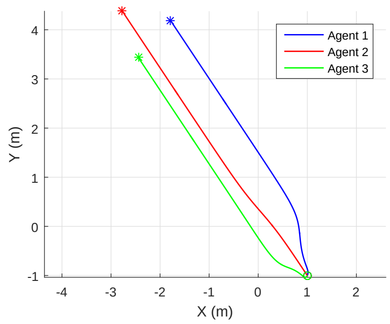

Fig. 1. Agent's trajectories when $\varepsilon = 0.1$ and all agents start at $(1, -1)$ at $t = 0$.

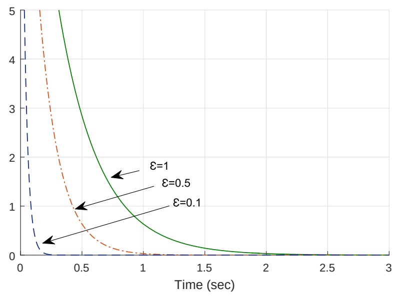

Fig. 2. Sum of the velocity error norms between the neighbor agents.

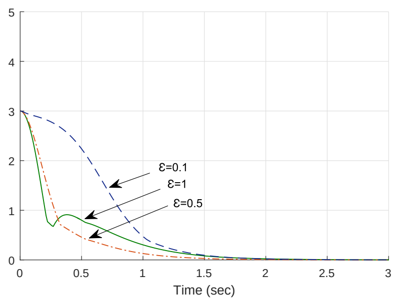

Fig. 3. Sum of the position error norms between the neighbor agents.

REFERENCES

Anderson, B.D.O., Yu, C., Fidan, B., and Hendrickx, J.M. (2008). Rigid graph control architectures for autonomous formations. *IEEE Control Systems*, 28(6).

Awad, A., Chapman, A., Schoof, E., Narang-Siddarth, A., and Mesbahi, M. (2018). Time-scale separation in networks: State-dependent graphs and consensus tracking. *IEEE Transactions on Control of Network Systems*.

Cao, Y., Ren, W., and Meng, Z. (2010). Decentralized finite-time sliding mode estimators and their applications in decentralized finite-time formation tracking. *Systems & Control Letters*, 59(9), 522–529.

Deghat, M., Anderson, B.D.O., and Lin, Z. (2016). Combined flocking and distance-based shape control of multi-agent formations. *IEEE Transactions on Automatic Control*, 61(7), 1824–1837.

Deghat, M., Shames, I., and Anderson, B.D.O. (2015). Safe autonomous agent formation operations via obstacle collision avoidance. *Asian Journal of Control*, 17(5), 1473–1483.

Dimarogonas, D.V. and Johansson, K.H. (2008). On the stability of distance-based formation control. In *Decision and Control, 2008. CDC 2008. 47th IEEE Conference on*, 1200–1205.

Hendrickx, J.M., Anderson, B.D.O., Delvenne, J.C., and Blondel, V.D. (2007). Directed graphs for the analysis of rigidity and persistence in autonomous agent systems. *International journal of robust and nonlinear control*, 17(10-11), 960–981.

Krick, L., Broucke, M.E., and Francis, B.A. (2009). Stabilisation of infinitesimally rigid formations of multi-robot networks. *International Journal of control*, 82(3), 423–439.

Loría, A. and Panteley, E. (2005). Cascaded nonlinear time-varying systems: Analysis and design. In *Advanced topics in control systems theory*, 23–64. Springer.

Mesbahi, M. and Egerstedt, M. (2010). *Graph theoretic methods in multiagent networks*. Princeton University Press.

Mou, S., Belabbas, M.A., Morse, A.S., Sun, Z., and Anderson, B.D.O. (2016). Undirected rigid formations are problematic. *IEEE Transactions on Automatic Control*, 61(10), 2821–2836.

Oh, K.K., Park, M.C., and Ahn, H.S. (2015). A survey of multi-agent formation control. *Automatica*, 53, 424–440.

Olfati-Saber, R. (2006). Flocking for multi-agent dynamic systems: Algorithms and theory. *IEEE Transactions on automatic control*, 51(3), 401–420.

Olfati-Saber, R., Fax, J.A., and Murray, R.M. (2007). Consensus and cooperation in networked multi-agent systems. *Proceedings of the IEEE*, 95(1), 215–233.

Qin, J., Zheng, W.X., and Gao, H. (2012). Coordination of multiple agents with double-integrator dynamics under generalized interaction topologies. *IEEE Transactions on Systems, Man, and Cybernetics, Part B (Cybernetics)*, 42(1), 44–57.

Ren, W., Beard, R.W., and Atkins, E.M. (2007). Information consensus in multivehicle cooperative control. *IEEE Control Systems*, 27(2), 71–82.

Sastry, S. (1999). *Nonlinear systems: analysis, stability, and control*, volume 10. Springer Science & Business Media.

Sun, Z., Anderson, B.D.O., Deghat, M., and Ahn, H.S. (2017). Rigid formation control of double-integrator systems. *International Journal of Control*, 90(7), 1403–1419.

Sun, Z., Helmke, U., and Anderson, B.D.O. (2015). Rigid formation shape control in general dimensions: an invariance principle and open problems. In *Proc. of the 2015 IEEE 54th Annual Conference on Decision and Control (CDC)*, 6095–6100. IEEE.

Sun, Z., Mou, S., Deghat, M., and Anderson, B.D.O. (2016). Finite time distributed distance-constrained shape stabilization and flocking control for d-dimensional undirected rigid formations. *International Journal of Robust and Nonlinear Control*, 26(13), 2824–2844.

Sun, Z. and Yu, C. (2017). Dimensional-invariance principles in coupled dynamical systems. *Submitted to IEEE Transactions on Automatic Control. Available at ArXiv preprint ArXiv:1703.07955.*

Tanner, H.G., Jadbabaie, A., and Pappas, G.J. (2007). Flocking in fixed and switching networks. *IEEE Transactions on Automatic control*, 52(5), 863–868.

Terrell, W.J. (2009). *Stability and stabilization: an introduction*. Princeton University Press.